A Carrier Magnitude Varying Modulation for Distributed Static Series Compensator to Achieve a Maximum Reactive Power Generating Capability

Yunting Liu and Fang Zheng Peng
Department of Electrical and Computer Engineering
Michigan State University
East Lansing, MI 48824 USA
liuyunti@msu.edu, fzpeng@egr.msu.edu

***Abstract*— Conventional single-phase H-bridge applications have second-order harmonic ripple power on the dc bus. However, in applications like a voltage source inverter (VSI) module of a Distributed Static Series Compensator (DSSC), a larger dc bus voltage fluctuation is acceptable since the dc bus connects to no load. This paper releases the constraints on dc bus voltage ripples so that the dc-bus capacitor can be fully utilized. Based on this idea, a carrier magnitude varying modulation is proposed, in which the VSI can generate ten times the reactive power of a conventional SPWM based VSI. The system reactive power generating capability is assessed to compare with the conventional SPWM based VSI and the constant duty cycle control based VSI. A PI controller is applied to the system to regulate the ac current. The analysis and design are validated by simulation and experiments.**

Keywords—dc capacitor; pulse width modulation; impedance control; H-bridge inverter

I. INTRODUCTION

The flexible ac transmission systems (FACTS) has been widely accepted to enhance the power grid stability, reliability, and controllability[1]-[5]. The power flow, P and Q, transmitted through a transmission line shown in Fig.1 is given by the expression:

$$P = \frac{V_1 V_2}{X_L}\sin(\delta_1 - \delta_2)\,,\ Q = \frac{V_1^2 - V_1 V_2}{X_L}\sin(\delta_1 - \delta_2) \qquad (1)$$

where V_1, and V_2 are the sending end and receiving end voltages, respectively. δ_1 and δ_2 are the sending end and receiving end voltage angle, respectively. X_L is the line impedance. The FACTS controls the power flow by manipulating these three variables (voltage, angle and impedance), selectively or concurrently [1]. A new type of FACTS device, called distributed series static compensator (DSSC), has been developed [2], [6]-[9]. DSSC generates/absorbs reactive power to manipulate the reactance of transmission line. In contrast to the large designs required of conventional FACTS and compensation solutions, DSSCs are small, modular units that can be installed and deployed as needed.

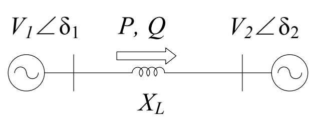

Fig.1. The DSSC structure.

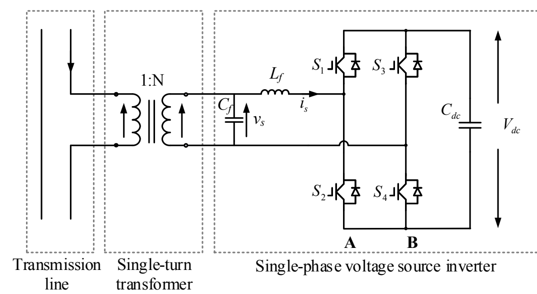

Fig.2. The DSSC structure.

The DSSC structure is shown in Fig.1[2]. The DSSC contains a single-turn transformer (STT) connected to a single-phase voltage source inverter (VSI), and is suspended from a transmission line. Since the STT inductance is fixed, it is the VSI operating range determines the DSSC's equivalent reactance range.

To generate reactive power in a conventional SPWM based single-phase inverter, the 2-ω voltage ripple on dc bus should be well limited within ±2.5% at steady state.

However, a constant dc-link voltage is not necessary for DSSC applications since the dc bus connects to no load. A constant duty cycle control has been proposed in [10]. It releases the constraint that the dc-link voltage should be relatively constant as the dc voltage of a conventional SPWM single-phase inverter. This method increases the maximum reactive power that the VSI can generate. However, the minimum reactive power that the VSI can generate also increases, which means there is a blind zone, between zero reactive power and the minimum reactive power, that the VSI cannot reach. This weakness becomes worse when the transmission line current increasing.

This paper proposed a carrier magnitude varying modulation for DSSC inverter that overcomes the weakness of the constant duty cycle control in terms of high power rating. The proposed method fills in the gap between zero reactive power and the minimum reactive power of the constant duty cycle control. Thus, the VSI reactive power capability is expanded.

II. DC-SIDE CAPACITOR INSTANTANEOUS POWER ANALYSIS

The following analysis examines the instantaneous power flow in the a VSI of the DSSC with conventional SPWM modulation. As shown in Fig. 3, the ac voltage u_s and current i_s are assumed to be sinusoidal and in a 90-degree phase difference as an ideal variable capacitor.

$$v_s(t) = \sqrt{2}V_s \cdot \sin(\omega t) \tag{1}$$

$$i_s(t) = \sqrt{2}I_s \cdot \cos(\omega t) \tag{2}$$

where V_s and I_s are the input voltage and current RMS values, respectively; and ω is the fundamental frequency. The instantaneous input power from the ac source can be expressed as follows:

$$p_s(t) = V_s I_s \cdot \sin(2\omega t) \tag{3}$$

As we can see in (3), the instantaneous power consists of only a ripple power, which will be completely absorbed by dc-bus capacitor and result in a 2-ω ripple voltage on dc bus. As seen from the Fig.3 (d), the dc voltage swings from its minimum value to the maximum value. The fluctuating part of the capacitor energy is defined as working energy (WE) whereas the constant part is defined as sleeping energy (SE).

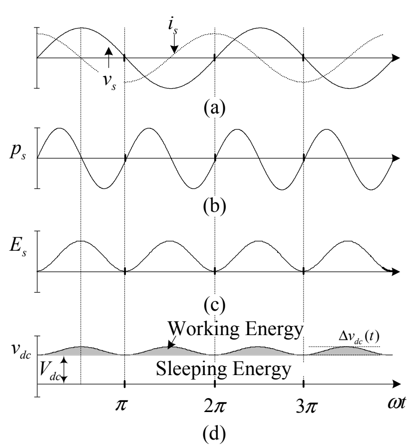

Fig.3. (a) input voltage and current; (b) instantaneous input power; (c) instantaneous input energy; and (d) dc-link capacitor voltage.

The definition can be formulated as

$$\begin{aligned} E_{dc}(t) &= \frac{1}{2}C_{dc} \cdot v_{dc}^2(t) \\ &= \underbrace{\frac{1}{2}C_{dc} \cdot V_{dc}^2}_{SE} + \underbrace{\frac{1}{2}C_{dc} \cdot \Delta v_{dc}^2(t) + C_{dc} \cdot \Delta v_{dc}(t) \cdot V_{dc}}_{WE(t)} \end{aligned} \tag{4}$$

Where C_{dc} is the dc capacitance; $v_{dc}(t)$ is the dc-bus voltage; V_{dc} is the constant part of dc-bus voltage; and $\Delta v_{dc}(t)$ is the ripple part of dc-bus voltage.

If dc-bus capacitor is at its minimum energy level when t = 0 as shown in Fig.3(d), the instantaneous input energy that flows into the dc-bus capacitor can be obtained by integrating (3)

$$E_s(t) = \frac{1}{2\omega} V_s I_s \cdot (1 - \cos(2\omega t)) \tag{5}$$

The relationship of equations (1)-(5) is illustrated in Fig. 3. The power balance holds true at any moment, i.e. the instantaneous input energy is equal to the working energy (WE) in (4). Then we can have the ripple voltage equation,

$$\Delta v_{dc}(t) = -V_{dc} + \sqrt{V_{dc}^2 + \frac{1}{\omega C_{dc}} \cdot V_s I_s \cdot (1 - \cos(2\omega t))} \tag{6}$$

A coefficient R is defined as the energy ratio. The definition can be written as

$$R = \frac{SE}{WE_{total}} \tag{7}$$

where WE_{total} is the maximum working energy in the dc capacitor in a fundamental cycle.

The higher the value of R is, the more sleeping energy there is in the system. For example, if a dc-bus voltage ripple of ±2.5% is allowed, the energy ratio of those applications is 9.25, which means 90.2% of the energy stored in the dc-bus capacitor is sleeping.

Assume the peak voltage of dc bus is equal to that of input voltage. $v_{dc}(t)$ can be derived as

$$v_{dc}(t) = V_{peak} \cdot \sqrt{\frac{R}{R+1} + \frac{1}{2(R+1)} \cdot (1 - \cos(2\omega t))} \tag{8}$$

To help visualize the dc-bus voltage in terms of R, Fig. 4 plots the dc-bus voltage with R = 20, R = 5, R = 1, R = 0.2 and R = 0 according to (8).

III. CARRIER MAGNITUDE VARYING MODULATION

This section discusses the modulation of the single-phase VSI under the condition that R is larger than zero and smaller than ten which includes the conventional SPWM VSI condition. [10] has only explained the modulation when R = 0. If combining the modulation of this section together with the one in [10], this will extremely extend the reactive power generating capability of the VSI.

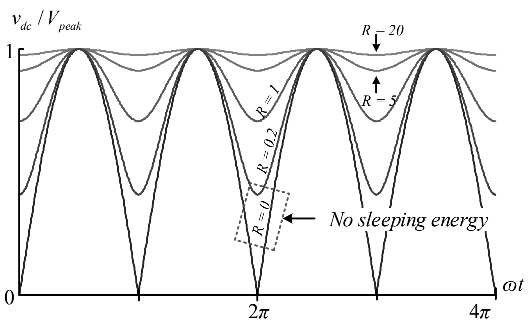

Fig.4 Dc-link capacitor voltage waveforms vs different energy ratios with a fixed peak voltage value.

Fig.5 shows all four possible switching states and the corresponding current paths of an H-bridge circuit. These four switching states could create three types of voltage across the mid-points (A and B in Fig.5), namely a) v_{AB} is positive, b) $v_{AB} = 0$, c) $v_{AB} = 0$, and d) v_{AB} is negative. The following analysis will only discuss the condition when v_s is positive, since the analysis would be similar when v_s is negative.

When v_s is positive, switching states from Fig.5(a) and (c) are selected as "effective switching states" to match with the required dc voltage. There are multiple ways to select effective switching states to generate the demanding dc voltage. This paper is only focusing on the aforementioned way of selecting effective switching states. Set S_3 to be off and S_4 to be on for the half period of a fundamental cycle when v_s is positive so that the negative side of the dc capacitor and the mid-point B can be shorted. S_1 and S_2 switch at a high frequency and create positive and zero potentials on mid-point A.

If ignoring the fundamental voltage drop on the filtering inductor L_f, the relationship between v_s and v_{dc} could be written as

$$v_{dc} D = v_s \tag{9}$$

where D is the duty-cycle of S_1 in a switching period.

(9) is the key equation to construct the proper PWM pulses. (9) can be decomposed into an equation set

$$\begin{cases} y = v_{dc}^* \cdot d \\ y = v_s^* \end{cases} \tag{10}$$

Fig. 6 shows how to construct the PWM pulses by converting (10) into graphs. v^*_{dc} is the expected v_{dc} value, or v_{dc} reference, and v^*_s is the expected v_s value. Note that the cross-point of the two straight lines is the solution of (10), which is the duty-cycle D. If repeating drawing Fig.6 in a period of 1 as illustrated in the dashed line, $y = v^*_{dc}d$ becomes a saw-tooth carrier while $y = v^*_s$ becomes the modulating signal. The minimum value of the saw-tooth carrier is zero and the maximum value of the saw-tooth carrier is v^*_{dc}.

The saw-tooth carrier shown in Fig. 6 is free and valid to be replaced by its triangular counterpart. A full picture of the modulation with triangular carrier is illustrated in Fig. 7. The envelope of the carrier is v^*_{dc} which was discussed in II. v^*_a is the modulating signal for the branch A of the VSI in Fig.2 and v^*_b is the modulating signal for the branch B of the VSI in Fig.2.

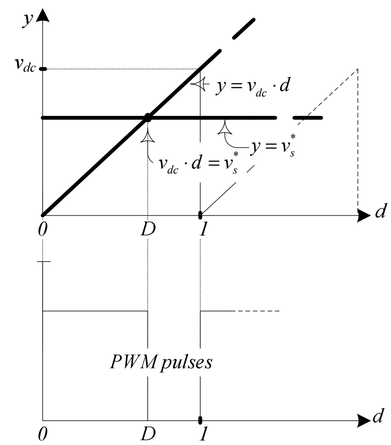

Fig.6. Construct the PWM pulses by converting key equation set (8) into graphs.

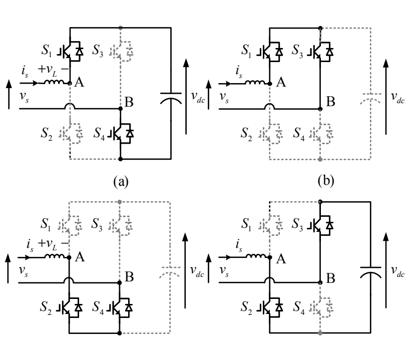

Fig.5. Four possible switching states and the corresponding current paths.

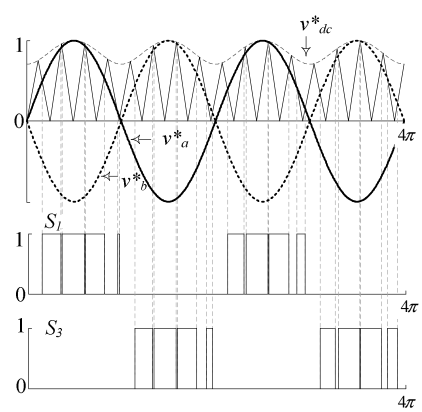

Fig.7. Modulation of the proposed carrier magnitude varying modulation.

IV. ASSESSMENT OF THE VSI EQUIVALENT REACTANCE RANGE

This section will compare the VSI equivalent reactance range and its reactive power generating capability under the condition of conventional SPWM modulation, the constant duty cycle control proposed in [10], and the carrier magnitude varying modulation proposed in this paper, to demonstrate the strength of the proposed method. The following comparison is based on the same system design. The only difference is the modulation strategy. In DSSC application, i_s is known and depending on the power flow of the transmission line.

In conventional SPWM modulation based VSI, it is the dc-bus voltage harmonic requirement limits the equivalent capacitance of the VSI. The relationship of the equivalent capacitance and Δv_{dc} could be written as

$$C_{eq}(\sqrt{2}V_s)^2 = C_{dc}V_{dc(\max)}^2 - C_{dc}(V_{dc(\max)} - \Delta v_{dc})^2 \tag{11}$$

Where $V_{dc(\max)}$ is the dc-bus peak voltage, and Δv_{dc} is the dc-bus voltage variation in each fundamental cycle. Since $V_s = I_s/(\omega C_{eq})$, re-write (11),

$$C_{eq} = \frac{2I_s^2}{\omega^2 C_{dc}\Delta v_{dc}\cdot(2V_{dc(\max)} - \Delta v_{dc})} \tag{12}$$

Since the equivalent reactance $X_{VSI(SPWM)} = -1/(\omega C_{eq})$, convert the C_{eq} into equivalent reactance,

$$X_{VSI(SPWM)} = \frac{-\omega C_{dc}\Delta v_{dc}\cdot(2V_{dc(\max)} - \Delta v_{dc})}{2I_s^2} \tag{13}$$

When $\Delta v_{dc} = 0$, $X_{VSI(SPWM)}$ reaches its maximum value, which is zero, whereas when Δv_{dc} at its maximum value, $X_{VSI(SPWM)}$ reaches its minimum value. For a SPWM modulated VSI, Δv_{dc} can reach up to 5% of the $V_{dc(max)}$.

The relationship of the reactive power generated by the VSI and its equivalent capacitance is $Q_{VSI} = I_s^2 X_{VSI}$. To demonstrate the reactive power generating capability of this method, calculate the reactive power,

$$Q_{VSI(SPWM)} = \frac{-\omega C_{dc}\Delta v_{dc}\cdot(2V_{dc(\max)} - \Delta v_{dc})}{2} \tag{14}$$

When $\Delta v_{dc} = 0$, $Q_{VSI(SPWM)}$ reaches its maximum value, which is zero, whereas when Δv_{dc} at its maximum value, $Q_{VSI(SPWM)}$ reaches its minimum value.

In constant duty cycle control based VSI, it is the dc-bus peak voltage requirement that limits the equivalent capacitance of the VSI, namely the maximum dc-bus voltage should be constraint to a practical value and the dc-bus voltage should be greater than v_s at any moment. The relationship of the equivalent capacitance and $V_{dc(\max)}$ could be written as

$$C_{eq}(\sqrt{2}V_s)^2 = C_{dc}V_{dc(\max)}^2 \tag{15}$$

Since $V_s = I_s/(\omega C_{eq})$, re-write (15),

$$C_{eq} = \frac{2I_s^2}{\omega^2 C_{dc}V_{dc(\max)}^2} \tag{16}$$

Since the equivalent reactance $X_{VSI(CDC)} = -1/(\omega C_{eq})$, convert the C_{eq} into equivalent reactance,

$$X_{VSI(CDC)} = -\omega C_{dc}V_{dc(\max)}^2/(2I_s^2) \tag{17}$$

When $V_{dc(max)}$ at its minimum value, which is $(\sqrt{2})I_s/(\omega C_{dc})$, $X_{VSI(CDC)}$ reaches its maximum value $-1/(\omega C_{dc})$, whereas when $V_{dc(max)}$ at its maximum value, $X_{VSI(SPWM)}$ reaches its minimum value.

Calculate the reactive power the VSI could generate,

$$Q_{VSI(CDC)} = -\omega C_{dc}V_{dc(\max)}^2/2 \tag{18}$$

When $V_{dc(max)} = (\sqrt{2})I_s/(\omega C_{dc})$, $Q_{VSI(CDC)}$ reaches its maximum value $-I^2/(\omega C_{dc})$, whereas when $V_{dc(max)}$ at its maximum value, $Q_{VSI(CDC)}$ reaches its minimum value.

In carrier magnitude varying modulation based VSI, the relationship of the equivalent capacitance and Δv_{dc} is the same as (12), which is the conventional SPWM capacitance. The difference of the SPWM one and the proposed carrier magnitude varying is that the proposed method allows a greater Δv_{dc} up to $V_{dc(max)}$. The equivalent reactance $X_{VSI(CMV)}$ is the same as (13). When $\Delta v_{dc} = 0$, $X_{VSI(CMV)}$ reaches its maximum value, which is zero, whereas when $\Delta v_{dc} = V_{dc(\max)}$, $X_{VSI(CMV)}$ reaches its minimum value $-1/(\omega C_{dc})$.

The relationship of the reactive power $Q_{VSI(CMV)}$ generated by the VSI is the same as (14). When $\Delta v_{dc} = 0$, $Q_{VSI(CMV)}$ reaches its maximum value, which is zero, whereas when $\Delta v_{dc} = V_{dc(\max)}$, $Q_{VSI(CMV)}$ reaches its minimum value $-I^2/(\omega C_{dc})$.

To compare the equivalent reactance and the reactive power capability of the VSI among aforementioned methods, assume that the dc-bus voltage peak value should not exceed $1.1\cdot(\sqrt{2})I_{s(max)}/(\omega C_{dc})$ for all three cases. Assume the conventional SPWM based VSI has a dc-bus voltage ripple of ±2.5%. Plot the equivalent reactance range and the reactive power capability in respect to I_s in Fig.8 and Fig.9. The carrier magnitude varying modulation completely covers the conventional SPWM method reactive power generating range and ties up with that of the constant duty cycle control.

V. CONTROL STRATEGY

Since the proposed DSSC single-phase VSI can be modeled as a variable capacitor when generating the reactive power, the VSI would interact with the filtering inductor L_f and lead to

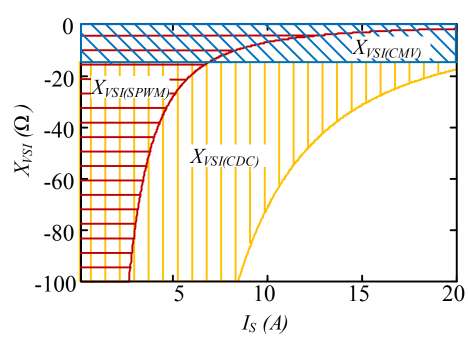

Fig.8. Equivalent reactance range in respect to input current I_s.

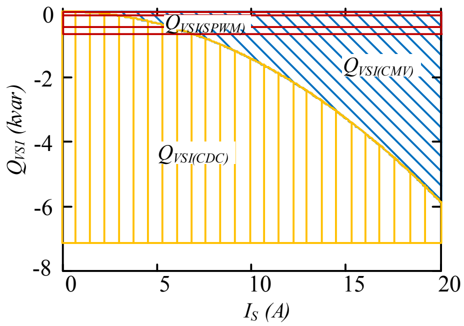

Fig.9. Reactive power generating capability vs input current I_s.

resonance on ac input current. In paper [10], a damping resistor is added to the circuit to damp the LC resonance. A current controller can remove the damping resistor, which simplify the circuit. A PI controller is constructed to regulate the input current and damp the LC resonance in this section. Fig. 10 shows the control system, which consists of input current control and feedforward for the input voltage reference.

VI. EXPERIMENT RESULTS

To verify the effectiveness of the proposed carrier magnitude varying modulation and its control strategy, a scaled down simulation and experiment are conducted. The passive components' parameters are summarized in Table I.

The schematic of the simulation and experimental prototype are illustrated as the VSI part of Fig.2. A 60-V voltage source is connected to the experimental circuit as the input. Fig.11 shows the simulation results of the proposed DSSC VSI generating a reactive power of (a) 125 var; (b) 250 var; and (c) 375 var. In Fig.11(c) the dc-bus voltage waveform become a folded sine-wave, which connects to the constant duty cycle control. The proposed DSSC VSI generates the reactive power correctly.

The experiment waveforms are shown in Fig. 12 while generating a reactive power of (a) 125 var; (b) 250 var; and (c) 375 var. Note that the LC resonance on input current i_s is damped by the close-loop control discussed in section V. The v_{dc} swings heavily in Fig.12(a) and Fig.(b) but never goes to zero. The dc-bus peak voltage is 90 V which is 1.1 times the input ac voltage peak value. Fig.12(c) shows the experiment result when R = 0. The v_{dc} goes to zero twice in a fundamental cycle in this condition. The DSP clock frequency is 60MHz. The total computation time including calculating dc-bus voltage reference and current control is less than 5 µs.

TABLE I. KEY PARAMETERS FOR A SINGLE-PHASE VAR GENERATOR

C_{dc}	L_f	v_s	Switching frequency	Fundamental frequency
180 μF	490 μH	60 V	20 kHz	60 Hz

VII. CONCLUSION

The carrier magnitude varying based DSSC VSI proposed in this paper fully utilizes the dc capacitor energy. The method helps overcome the weakness of a constant duty cycle modulated VSI at high power rating. The proposed method fills in the gap between the conventional SPWM modulation and the constant duty cycle control so the VSI can smoothly operate between SPWM modulation and the constant duty cycle control and benefit from the strengths of both methods. Thus, the DSSC VSI achieves a maximum reactive power generating capability.

REFERENCES

[1] L. Gyugyi, C. D. Schauder, and K. K. Sen, "Static synchronous series compensator: A solid-state approach to the series compensation of transmission lines," *IEEE Trans. Power Del.*, vol. 12, no. 1, pp.406–417, Jan. 1997.

[2] D. Divan and H. Johal, "Distributed FACTS-A new concept for realizing grid power flow control," *IEEE Trans. Power Electron.*, vol. 22, no. 6, pp. 2253–2260, Nov. 2007.

[3] Z. Yuan, S. W. H. de Haan, J. B. Ferreira, and D. Cvoric, "A FACTS device: Distributed power-flow controller (DPFC)," *IEEE Trans. Power Electron.*, vol. 25, no. 10, pp. 2564–2572, Oct. 2010.

[4] F. Z. Peng, S. Zhang, S. Yang, D. Gunasekaran, and U. Karki, "Transformer-less unified power flow controller using the cascade multilevel inverter," in *Proc. Int. Power Electron. Conf.*, May 2014, pp. 1342–1349.

[5] H. Akagi, S. Inoue, and T. Yoshii, "Control and performance of a transformerless cascade PWM STATCOM with star configuration," *IEEE Trans. Ind. Appl.*, vol. 43, no. 4, pp. 1041–1049, Jul./Aug. 2007.

[6] D. Divan and H. Johal, "Distributed FACTS - A New Concept for

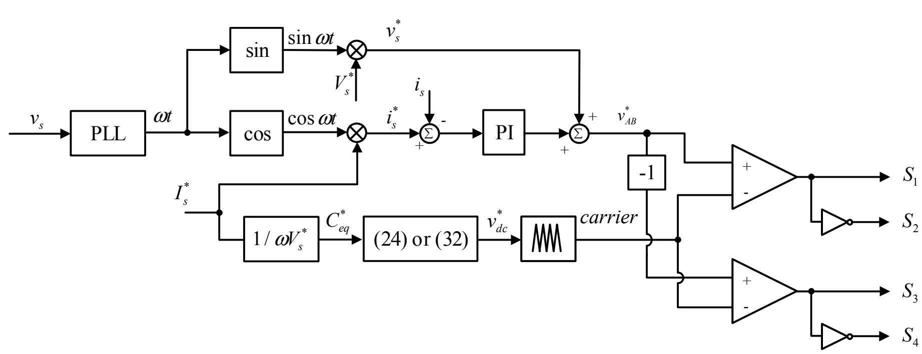

Fig.10. Reactive power generating capability in terms of Is.

Realizing Grid Power Flow Control," IEEE 2005 *Power Electronics Specialists Conf.*, Recife, Brasil, pp. 8-14.

[7] F. Kreikebaum, M. Imayavaramban, D. Divan, "Active Smart Wires: An Inverter-less Static Series Compensator," IEEE 2010 *Energy Conversion Congr. and Expo.*, Atlanta, GA, pp.3626-3630.

[8] F. Kreikebaum, D. Das, D. Divan, "Reducing transmission investment to meet Renewable Portfolio Standards using Controlled Energy Flows," IEEE 2010 *Innovative Smart Grid Technologies*, Gaithersburg, MD, pp.1-8.

[9] H. Johal, D. Divan, "Design Considerations for Series-Connected Distributed FACTS Converters," *IEEE Trans. Ind. Appl.*, vol.43, no.6, pp.1609,1618, Nov./Dec. 2007.

[10] A. Brissette, A. Hoke and D. Maksimović, "A constant duty cycle control, single-phase inverter design for distributed static series compensators," *2015 IEEE Applied Power Electronics Conf. and Expo.*, Charlotte, NC, 2015, pp. 1787-1794.

[11] Y. Liu and F. Z. Peng, "Real DC capacitor-less active capacitors," *2017 IEEE Applied Power Electronics Conf. and Expo.*, Tampa, FL, 2017, pp. 44-51.

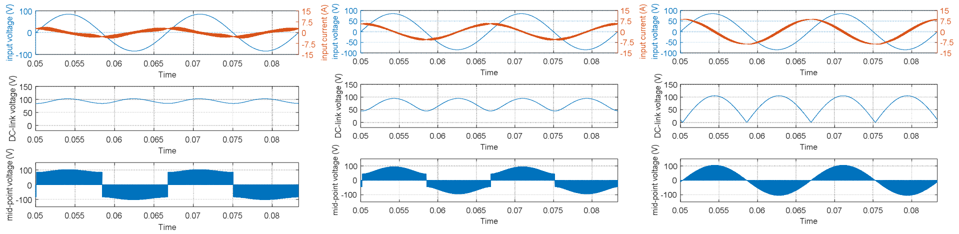

(a) (b) (c)

Fig.11. The experiment results of the proposed H-bridge VAr generator when generating a reactive power of (a) 125 var ($C_{eq} = 0.5C_{dc}$); (b) 250 var ($C_{eq} = C_{dc}$); (c) 375 var ($C_{eq} = 1.5 C_{dc}$); and (d) 500 var ($C_{eq} = 2C_{dc}$).

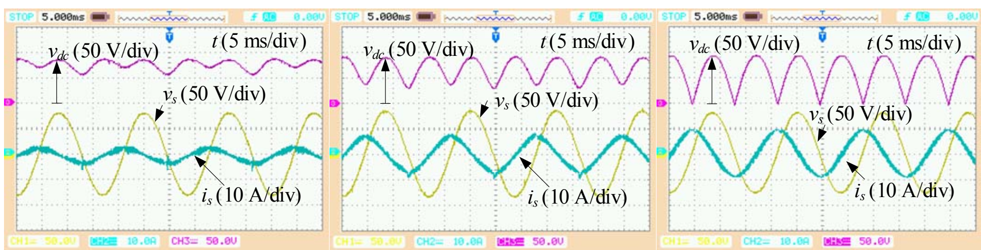

(a) (b) (c)

Fig.12. The experiment results of the proposed H-bridge VAr generator when generating a reactive power of (a) 125 var ($C_{eq} = 0.5C_{dc}$); (b) 250 var ($C_{eq} = C_{dc}$); (c) 375 var ($C_{eq} = 1.5 C_{dc}$); and (d) 500 var ($C_{eq} = 2C_{dc}$).